Supplementary Figures

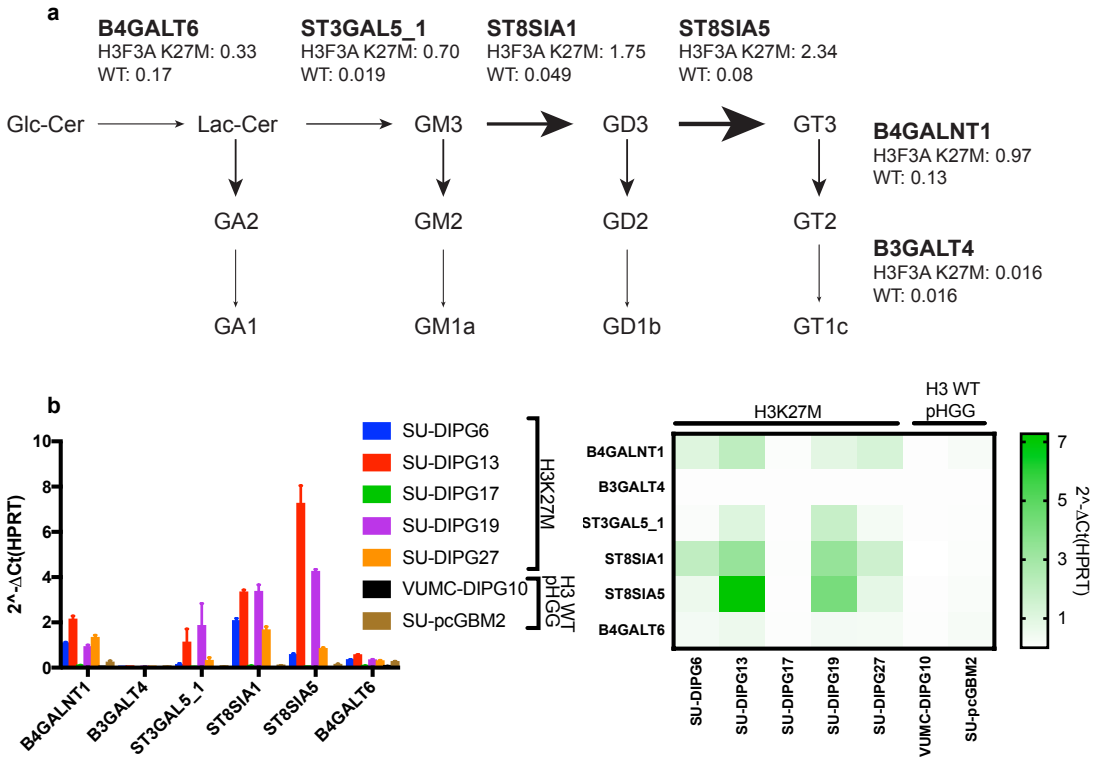

Supplementary Figure 1. **Pathway analysis of ganglioside enzyme gene expression**. Transcription of target ganglioside synthesis pathway enzymes was assessed by semiquantitative RT-PCR (**a**). In the biosynthesis flow diagram, the average expression value ($2^{-dCt(HPRT)}$ of key pathway enzymes (genes in boldface) across each culture of the given genotype is shown, and the arrow size is scaled to the average expression in *H3F3A* K27M cultures. Across the majority of *H3F3A* K27M cultures, expression of ganglioside synthesis enzymes upstream of GD2 is substantially increased compared to H3 WT pediatric high-grade glioma (pHGG) cultures. Across all *H3F3A* K27M cultures, *B3GALT4* expression is minimal compared to upstream genes, suggesting potentially limited rates of GD2 to GD1b conversion. (**b**) Heatmap and bar graph representation of expression values for individual cultures in each H3 genotype category (n=3 replicate culture samples for each line with technical duplicate reactions, statistical testing included culture replicates only). Primers utilized for qPCR expression analysis are given in Supplementary Table 3.

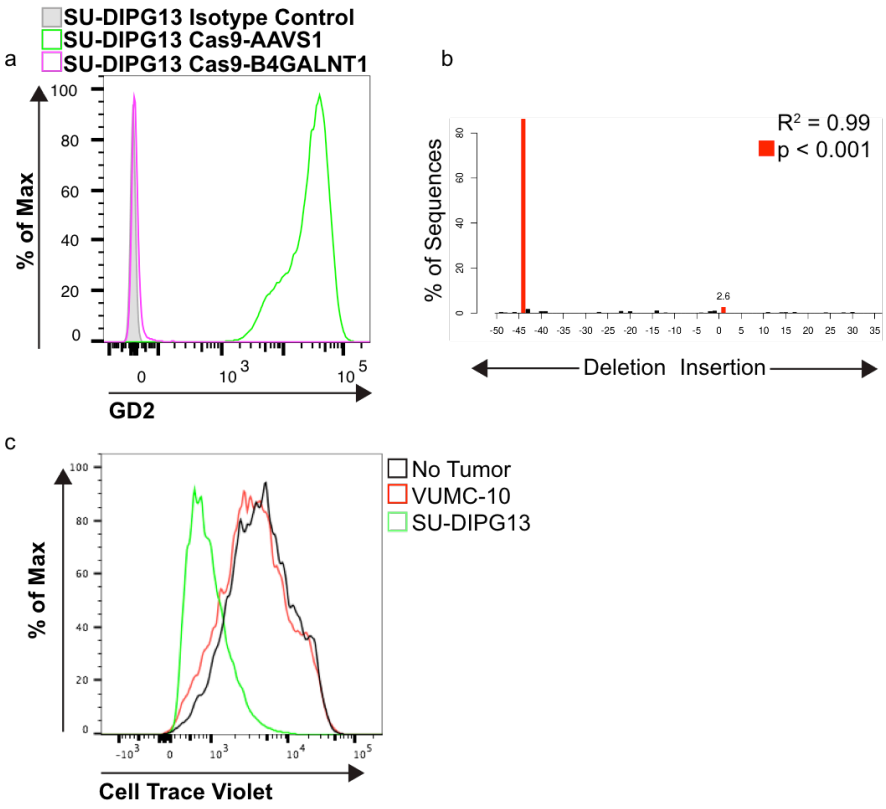

Supplementary Figure 2. Cas9-mediated deletion of GD2 synthase eliminates GD2 expression in DIPG cultures. (a) SU-DIPG13 cells electroporated with Cas9-gRNA complexes eliminates GD2 surface expression (b) following an ~45bp deletion at the gRNA target site (two-tailed T test of variance-covariance matrix of standard errors between modeled indel traces and parent sequence, implemented in Tracking of Indels by Decomposition webtool, tide-calculator.nki.nl). As a control, gRNA targeting the AAVS1 locus were used. (c) Cell Trace Violet proliferation assay performed on GD2-CAR T cells following in vitro incubation with the GD2-negative line VUMC-10 or GD2-high SU-DIPG13 demonstrated antigen-specific proliferation of GD2-CAR T cells. Experiments in (a) and (c) where independently repeated twice.

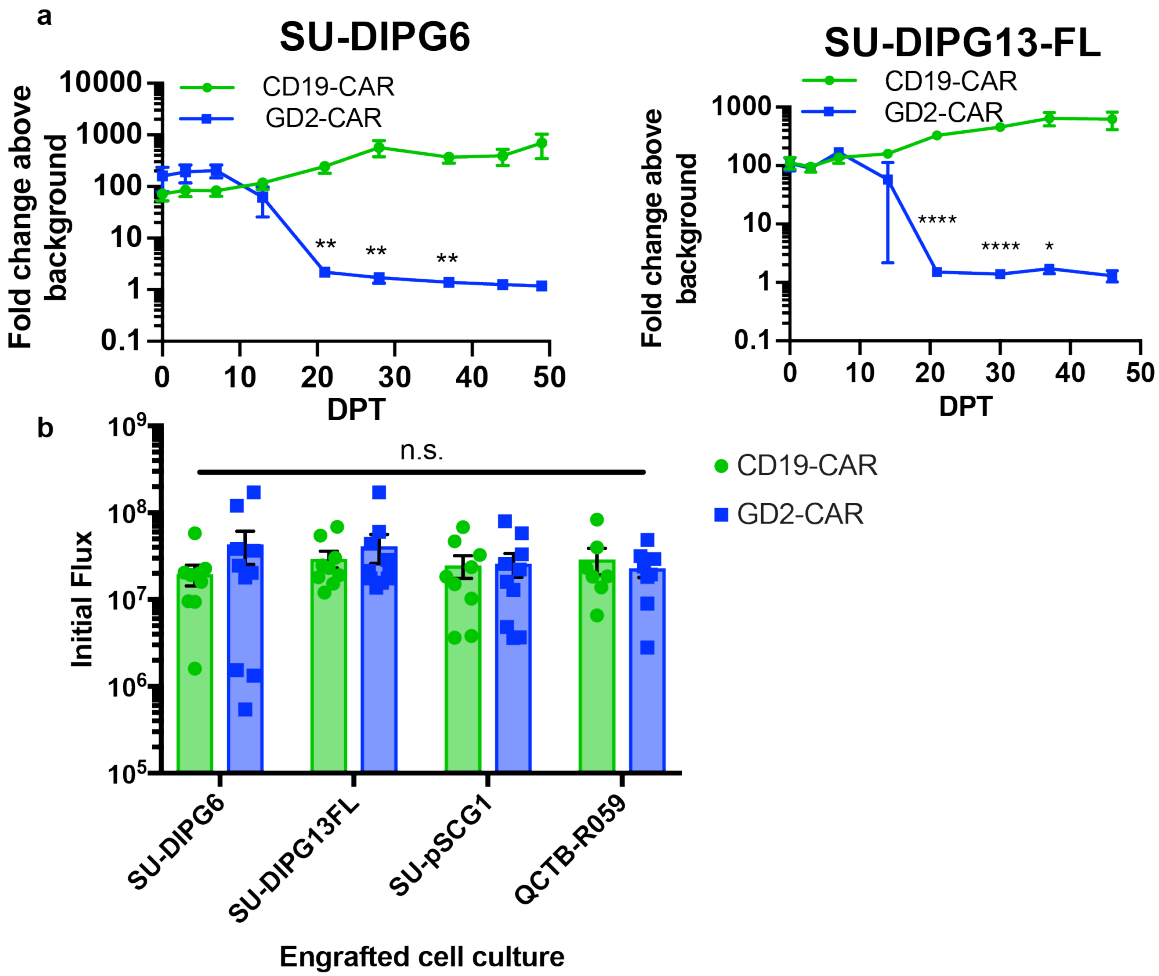

Supplementary Figure 3. Single intravenous dose of GD2-CAR T cells clear luciferase-expressing patient-derived DIPG xenografts to background bioluminescence levels. (a) SU-DIPG6 and SU-DIPG13FL xenograft tumor burden was monitored by in vivo bioluminescence imaging (Fig 2). To assess whether tumor clearance was complete by this measure, matched region of interest (ROI) measurements of total flux were made over the tumor-bearing region and an uninvolved area of the animal's flank. Fold change above background was then computed as the ratio of tumor ROI flux to background ROI flux (SU-DIPG6 n=10 CD19-CAR, 11 GD2-CAR; SU-DIPG13-FL n=13 CD19-CAR, 14 GD2-CAR). A ratio of 1 therefore indicates clearance of tumor luminescence signal to background levels, which was achieved in both models by DPT40 (* = $p<0.05$, ** = $p<0.01$, *** = $p<0.0001$, 2-tailed Student's t test with Holm-Sidak correction for multiple comparisons). (b) No statistically significant difference in initial tumor burden as assessed by in vivo bioluminescence imaging existed between animals in CD19-CAR or GD2-CAR treated cohorts of SU-DIPG6, SU-DIPG13FL, or additional H3K27M+ DMG cultures SU-pSCG1 and QCTB-R059 (Fig 4, two-way ANOVA with Tukey correction for multiple comparisons, n.s. = not significant at $\alpha=0.05$). Scatter points indicate individual mice, bars indicate mean, and error bars indicate SEM.

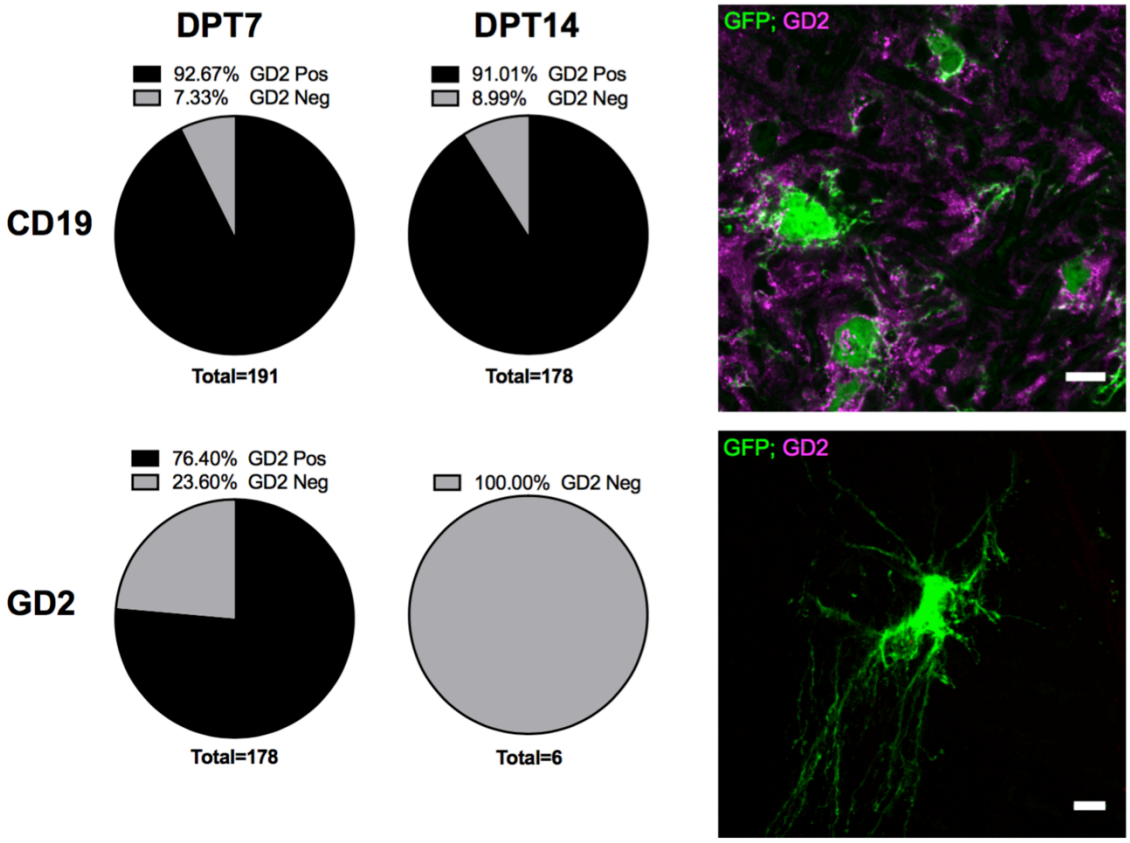

Supplementary Figure 4. Selective pressure of GD2 CAR T cell therapy in DIPG xenografts. Immunofluorescent staining for GD2 (clone 14g2a) in CD19 or GD2-CAR T cell-treated SU-DIPG13FL xenografts demonstrates selective pressure of GD2-CAR T cell therapy during the acute phase of tumoricidal activity. By DPT14, when the vast majority of parenchymal tumor has been cleared in GD2 CAR T cell-treated animals, the small number of remaining GFP+ tumor cells do not co-stain for GD2. Scale bar represents 10 microns. Total n given for each chart indicates number of cells assessed across 2 animals for each CAR/timepoint combination.

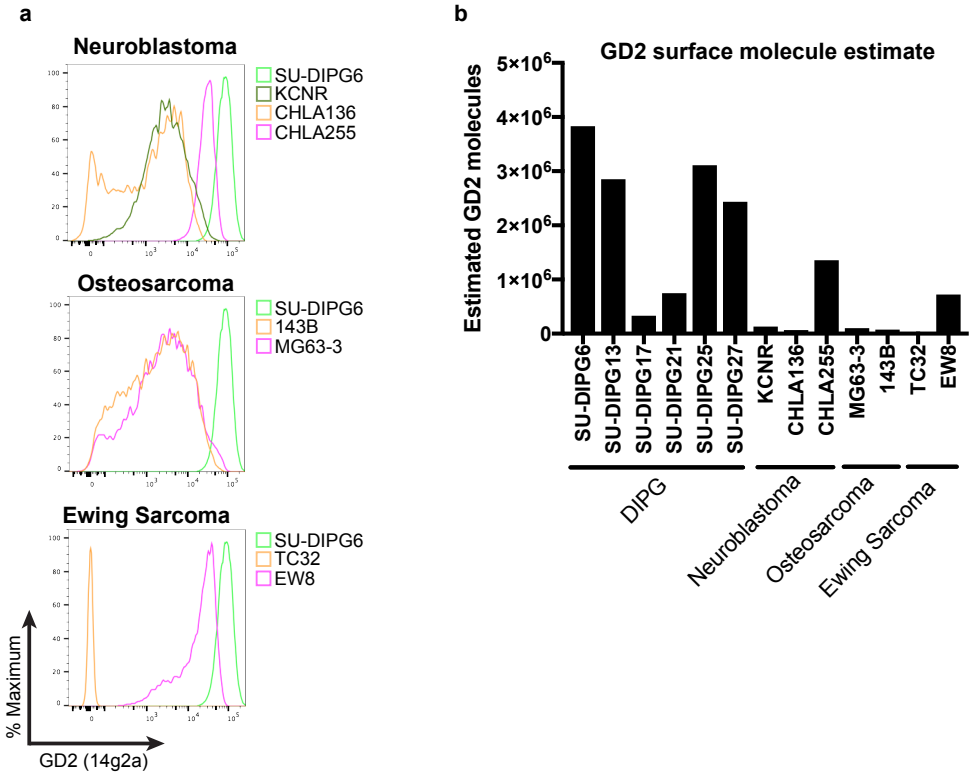

Supplementary Figure 5. DIPG cultures express GD2 at homogenously high levels relative to other GD2-positive tumor cell lines. (a) Flow cytometry staining for GD2 (clone 14g2a) on the surface of DIPG cultures revealed stronger and more uniform expression relative to cells derived from other malignancies under investigation for GD2-targeting immunotherapies, including neuroblastoma (KCNR, CHLA136, CHLA255), osteosarcoma (143B, MG63-3), and Ewing sarcoma (TC32, EW8). (b) Quantitative estimates of GD2 surface expression were obtained using fluorescent bead standards (Quantibrite, BD) for DIPG and other cancer lines. Flow cytometry stains were independently repeated twice.

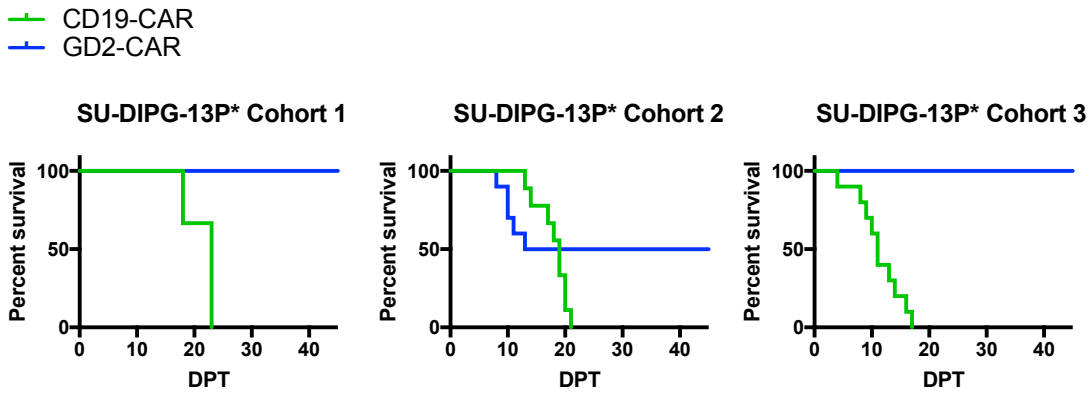

Supplementary Figure 6. Survival analysis across three independent cohorts of DIPG-13P*. Survival benefit of GD2 CAR T cell therapy was assessed in three independent cohorts of SU-DIPG13P* xenografts. Combined cohort data and statistical analysis is presented in Figure 3. In 1/3 cohorts (Cohort 2), several deaths in GD2 CAR T cell-treated animals were observed acutely, from DPT8-13. Animal numbers were as follows: Cohort 1 n=3 CD19-CAR, 5 GD2-CAR, Cohort 2 n=9 CD19-CAR, 10 GD2-CAR, Cohort 3 n=10 CD19-CAR, 9 GD2-CAR.

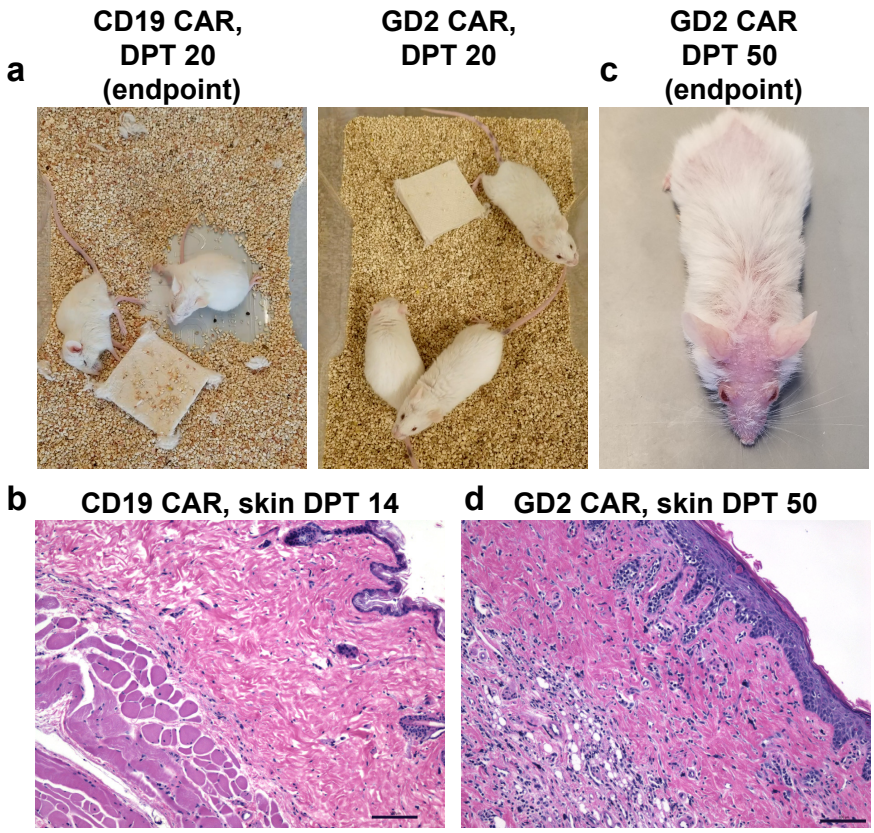

Supplementary Figure 7. Onset of xenogeneic graft-versus-host disease limits duration of monitoring in GD2-CAR T cell-treated patient derived xenograft models. Adoptive transfer of human T cells to NSG mice has been shown to result in graft versus host disease. (**a**) In SU-DIPG13P* xenografts, mice treated with CD19-CAR T cells display extensive signs of neurological impairment at endpoint consistent with tumor progression, including paralysis and aberrant motor behavior; however, classical signs of GvHD such as hair loss are absent at this timepoint. At this timepoint, animals treated with GD2-CAR T cells appear normal (**b**) Hematoxylin/eosin staining of skin specimens from CD19 CAR-treated animals at DPT14 appear grossly normal. (**c**) By DPT50, GD2-CAR treated animals exhibit extensive hair loss, and (**d**) hematoxylin/eosin staining of skin specimens reveals extensive lymphocytic infiltrate of dermis and epidermal hyperplasia, consistent with the onset of GvHD. Scale bars for H&E images are 100um, and staining was performed twice.

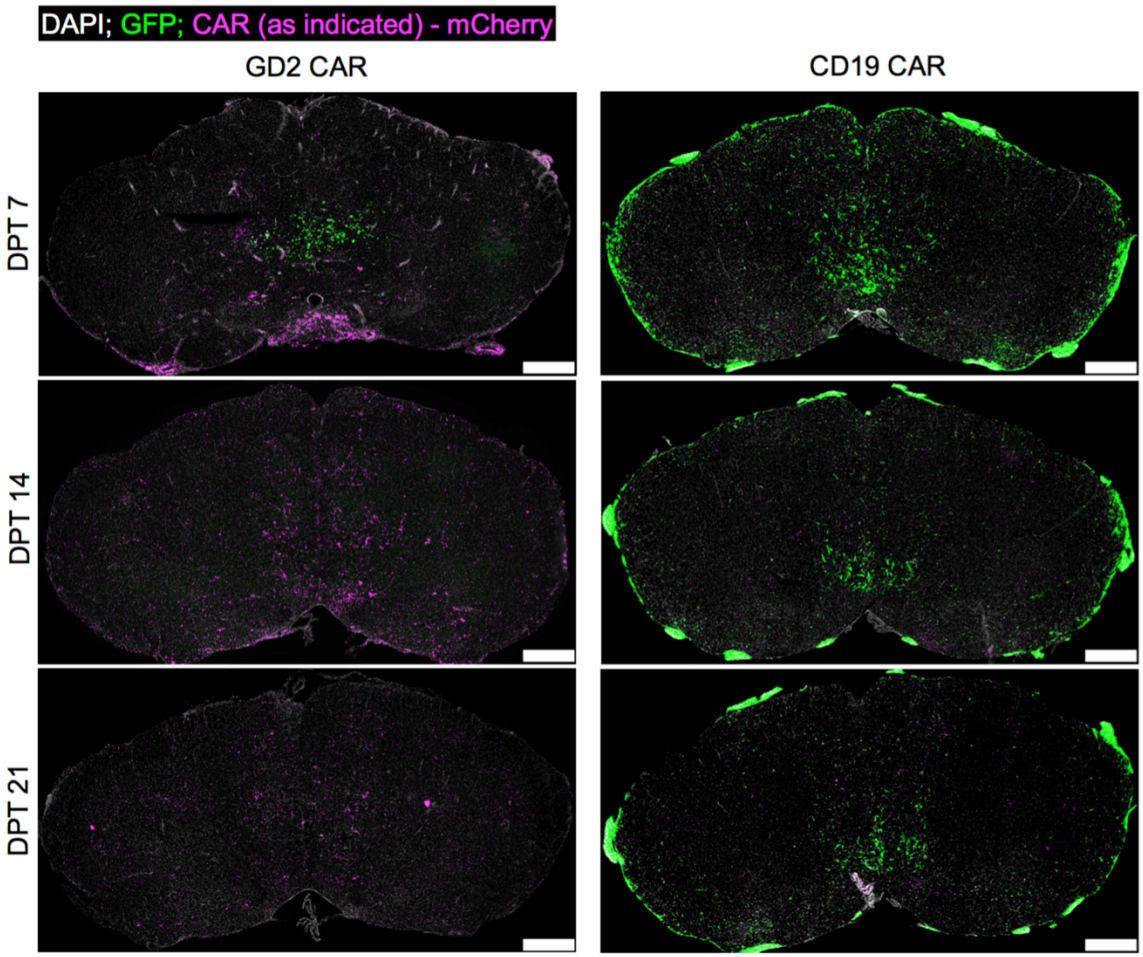

Supplementary Figure 8. Labeled GD2 CAR T cells invade tumor site during period of antitumor activity. Human T cells bearing a CAR fused at the C-terminus with mCherry were tracked in histological specimens of DIPG xenografts euthanized at the indicated timepoints. DIPG13-FL stably transduced with a lentiviral GFP-luciferase construct were engrafted into the pons of P2 NSG mice and treated with a single intravenous dose of $1X10^7$ GD2-CAR-mCherry or CD19-CAR-mCherry T cells. Bioluminescence imaging was used to randomize animals with equivalent initial tumor burden into GD2- or CD19-CAR groups. Representative fluorescence micrographs of medullary tumor burden are shown here. GD2-CAR-mCherry T cells infiltrate the tumor parenchyma as early as DPT7. By this timepoint, meningeal tumor has been cleared in the GD2-CAR-mCherry group but parenchymal tumor burden remains. By contrast, CD19-CAR-mCherry T cells do not achieve significant tumor clearing, although scattered CD19-CAR-mCherry cells can be identified within the tissue parenchyma. DPT7 and 14 images from GD2-CAR-mCherry animals are presented in Fig 3h; they are shown again here for comparison with matched CD19-CAR-mCherry images. Scale bar represents 500um. Experiment was repeated independently twice.

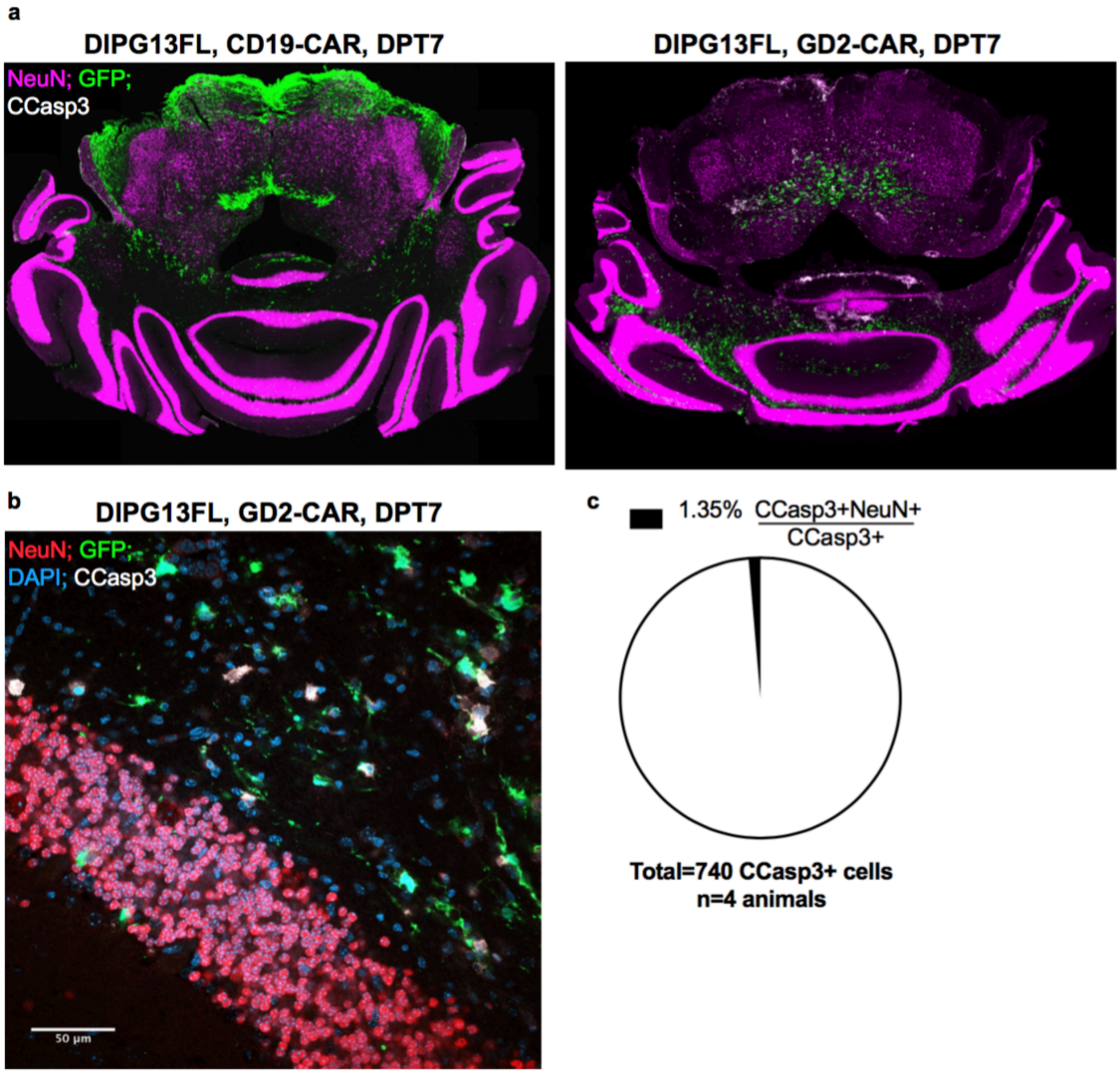

Supplementary Figure 9. Cleaved caspase-3 staining of GD2-CAR T cell treated DIPG xenografts. (a) Immunofluorescence microscopy of DIPG13-FL xenografts treated with a single intravenous dose of GD2-CAR T cells, euthanized at DPT 7 and stained for the neuronal marker NeuN and the apoptosis marker cleaved caspase 3 (CCasp3). (b) Immunofluorescence micrograph of antitumor activity in the cerebellum demonstrating intact granule layer neurons in the presence of local antitumor activity. (c) Out of the total population of CCasp3+ cells identified in GD2-CAR T cell-treated xenografts, <2% co-stain for NeuN (n=4 GD2-CAR treated animals, 740 total CCasp3+ cells assessed). Staining was performed in 4 independent mice.

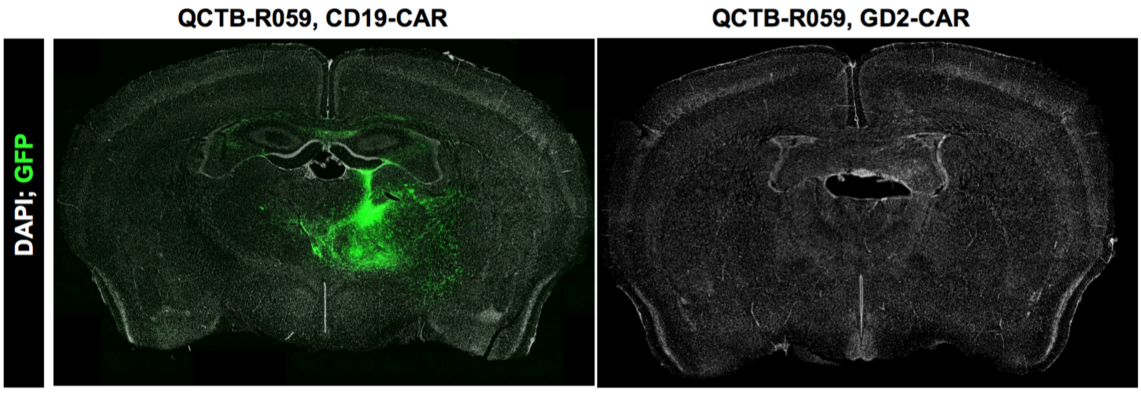

Supplementary Figure 10. GD2 CAR-T cell therapy achieves histological clearance of tumor burden in surviving QCTB-R059 thalamic H3K27M xenografts. Representative images from CD19 and GD2-CAR T cell treated animals demonstrate clearance of GFP-expressing tumor cells. No region of substantial residual tumor burden could be identified. Staining was performed in two independent mice.

Supplementary Table 2: Cell culture STR fingerprinting

		STR Fingerprint									
Cell Culture	**Histone Status**	AMEL	CSF1PO1	D13S317	D16S539	D21S11	D5S818	D7S820	TH01	TPOX	vWA
SU-DIPG6	H3F3A K27M	X/X	10/11	11/	8/13	29/31	10/12	8/9	7/8	8/11	17/18
SU-DIPG13	H3F3A K27M	X/ X	9/10	11/12	11/12	30/ OL (overload)	12/12	9/9	6/7	OL/8	13/18
SU-DIPG17	H3F3A K27M	X/ Y	13/13	9/9	9/12	28/29	11/11	8/9	7/7	8/11	18/19
SU-DIPG19	H3F3A K27M	X/ Y	10/11	13/14	9/13	30/30	11/12	10/10	9.3/9.3	8/11	17/18
SU-DIPG21	HIST1H3B K27M	X/ Y	11/12	8/13	10/10	30/32	10/11	8/9	6/6	8/12	16/19
SU-DIPG25	H3F3A K27M	X, X	12, 12	8, 11	12, 13	30, 35	11, 13	10, 12	9 ,9	7, 8	14, 18
SU-DIPG27	H3F3A K27M	X, Y	11, 12	9, 12	10, 12	30, 33.2	11, 11	9, 12	6, 6	8, 11	16, 17
SU-DIPG33	HIST1H3B K27M	X, Y	11, 12	8, 10	10, 12	30, 30	10, 12	10, 12	8, 9	8, 11	14, 14
SU-DIPG35	H3F3A K27M	X, X	10, 12	12, 13	9, 12	31.2, 32.2	12, 12	10, 13	6, 7	8, 8	15, 16
VUMC-DIPG10	H3 WT	X, X	10, 11	13, 13	11, 12	30,30	10, 13	12, 12	7, 9	8, 11	15, 19
SU-pcGBM2	H3 WT	X/Y	10/11	11/	9/11	28/30.2	11/	11/12	9.3/	8/12	17/18
SU-pSCG1	H3F3A K27M	X/Y	10/12	12/	11/12	28/29	11/12	10/	9.3/	8/11	16/18
QCTB-R059	H3F3A K27M	X/X	12,13	12/	11/	29,31.2	12/	8,11	9/	11,13	13,16

Supplementary Table 3: Primers used for RT-PCR

B4GALNT1	ACTGGTCACTTACAGCAGCC	GCGGGTGTCTTATGCGGATA
B3GALT4	GGTTTTGCACAGCGAGGAAG	AGGCCACTGCTCCTCTGATA
ST3GAL5_1	CACACCCTGAACCAGTTCGA	TCAAGGTCAGACAGTGGTGC
ST8SIA1	AGAGCATGTGGTATGACGGG	ATCCCACCATTTCCCACCAC
ST8SIA5	ATTAAGAGAGGCCTCCAGTTTG	CCTCAGCTCCAGGCATCTTG
B4GALT6	CCATACCTCCCCTGTCCAGA	CAATGACCCCCTGGCTCAAT
HPRT1	CTGGCGTCGTGATTAGTGAT	TCTCGAGCAAGACGTTCAGT